

NASA Contractor Report 187611
ICASE Report No. 91-65

ICASE

DEVELOPMENT OF TURBULENCE MODELS FOR SHEAR FLOWS BY A DOUBLE EXPANSION TECHNIQUE

V. Yakhot
S. Thangam
T. B. Gatski
S. A. Orszag
C. G. Speziale

Contract No. NAS1-18605
July 1991

Institute for Computer Applications in Science and Engineering
NASA Langley Research Center
Hampton, Virginia 23665-5225

Operated by the Universities Space Research Association



National Aeronautics and
Space Administration

Langley Research Center
Hampton, Virginia 23665-5225

CR-187611 DEVELOPMENT OF TURBULENCE
MODELS FOR SHEAR FLOWS BY A DOUBLE EXPANSION
TECHNIQUE Final Report (ICASE) 27 p
CSCL 200 G3/34 Unclass 0037365



DEVELOPMENT OF TURBULENCE MODELS FOR SHEAR FLOWS BY A DOUBLE EXPANSION TECHNIQUE

V. Yakhot*, S. Thangam^{††}, T. B. Gatski[§],
S. A. Orszag* and C. G. Speziale[†]

*Applied & Computational Mathematics, Princeton University, Princeton, NJ 08544

[†]ICASE, NASA Langley Research Center, Hampton, VA 23665

[§]NASA Langley Research Center, Hampton, VA 23665

ABSTRACT

Turbulence models are developed by supplementing the renormalization group (RNG) approach of Yakhot & Orszag with scale expansions for the Reynolds stress and production of dissipation terms. The additional expansion parameter ($\eta \equiv \bar{SK}/\bar{E}$) is the ratio of the turbulent to mean strain time scale. While low-order expansions appear to provide an adequate description for the Reynolds stress, no finite truncation of the expansion for the production of dissipation term in powers of η suffices – terms of all orders must be retained. Based on these ideas, a new two-equation model and Reynolds stress transport model are developed for turbulent shear flows. The models are tested for homogeneous shear flow and flow over a backward facing step. Comparisons between the model predictions and experimental data are excellent.

[†]Permanent Address: Stevens Institute of Technology, Hoboken, NJ 07030.

[†]This research was supported by the National Aeronautics and Space Administration under NASA Contract No. NAS1-18605 while the authors were in residence at the Institute for Computer Applications in Science and Engineering (ICASE), NASA Langley Research Center, Hampton, VA 23665.

I. Introduction

According to the Kolmogorov theory¹ of turbulence, the dynamics of velocity fluctuations $\mathbf{v}(\mathbf{k}, \omega)$ at the scale $l = 2\pi/k$ depend only on the mean rate of dissipation of kinetic energy $\bar{\mathcal{E}}$ and the length scale l . Neither the integral (L) nor dissipation ($l_d = 2\pi/k_d$) scales enter the dynamics of the inertial range of scales where $l_d \ll l \ll L$. Based on this theory, the velocity of eddies of size l scales as $\bar{\mathcal{E}}^{1/3}l^{1/3}$ so that the characteristic (turnover) time of these eddies is

$$T(l) \simeq \frac{l}{v(l)} \simeq \bar{\mathcal{E}}^{-1/3}l^{2/3}. \quad (1)$$

The velocity correlation function can then be represented in the scaling form

$$\langle v_i(\mathbf{k}, \omega)v_i(\mathbf{k}', \omega') \rangle \simeq k^{-13/3}\phi\left(\frac{\omega}{\bar{\mathcal{E}}^{1/3}k^{2/3}}\right) \equiv C(k, \omega) \quad (2)$$

where the scaling function $\phi(x)$ is to be determined from other considerations. The energy spectrum $E(k)$ is of the form

$$E(k) \simeq k^2 \int C(k, \omega) d\omega = C_K \bar{\mathcal{E}}^{2/3} k^{-5/3} \quad (3)$$

where C_K is the so called Kolmogorov constant. These results also yield the effective (turbulent) viscosity ν_T at the scale $l = 2\pi/k$:

$$\nu_T(k) \simeq v_l l \simeq \bar{\mathcal{E}}^{1/3} k^{-4/3}. \quad (4)$$

This effective viscosity plays a profound role in turbulence modelling. For example, it is quite reasonable to assume that the large-scale properties of the flow are governed by effective equations of motion similar to the Navier-Stokes equations with the effects of strong interactions between the velocity fluctuations taken into account through an effective viscosity (see Yakhot and Orszag²)

$$\nu_T \simeq \bar{\mathcal{E}}^{1/3} L^{4/3}. \quad (5)$$

However, the strict notion of eddy viscosity requires the existence of a small parameter $l/L \ll 1$ which is absent in turbulent flow. Still, the eddy viscosity concept proves to be extremely useful, working much better than expected. This situation is not unique: in a fluid close to thermal equilibrium, the molecular viscosity representation is very accurate even when the mean free path λ is not that small ($\lambda/L \simeq 1$).

Many years before Kolmogorov's work, Osborne Reynolds realized that turbulent flow was a random system which had to be treated using statistical methods. The work of Reynolds was similar in concept to the work of Boltzmann, Gibbs and others who formulated the

kinetic theory of gases. It was not an accident that by the early 20th century the ideas of kinetic theory were adapted to describe turbulence with turbulent eddies as the molecules or building blocks of this “gas.” By analogy with kinetic theory the turbulent viscosity is taken to be:

$$\nu_T \simeq u_{rms} L. \quad (6)$$

Combining (6) with (5) and using $\bar{\mathcal{E}} \simeq u_{rms}^3 / L$ (so that, in the absence of turbulence production, the turbulence is damped in one large-eddy turnover time L/u_{rms}), we obtain the $\bar{K} - \bar{\mathcal{E}}$ model:

$$\nu_T = C_\mu \frac{\bar{K}^2}{\bar{\mathcal{E}}} \quad (7)$$

where $\bar{K} = \frac{1}{2} \bar{u}_i \bar{u}_i$ and C_μ is a constant. The relation (7) is more convenient than (6) since it expresses the turbulent viscosity through the directly measurable quantities \bar{K} and $\bar{\mathcal{E}}$.

To implement (7) we need equations of motion for K , \mathcal{E} and the velocity field \mathbf{v} :

$$\frac{\partial \mathbf{v}}{\partial t} + \mathbf{v} \cdot \nabla \mathbf{v} = -\nabla p + \nu_0 \nabla^2 \mathbf{v} \quad (8)$$

$$\frac{\partial K}{\partial t} + \mathbf{v} \cdot \nabla K = -\mathcal{E} - \nabla_i (v_i p) + \nu_0 \nabla^2 K \quad (9)$$

$$\frac{\partial \mathcal{E}}{\partial t} + \mathbf{v} \cdot \nabla \mathcal{E} = -T_1 - T_2 - 2\nu_0 (\nabla_j v_i) (\nabla_i \nabla_j p) + \nu_0 \nabla^2 \mathcal{E} \quad (10)$$

where p is the pressure and

$$\begin{aligned} T_1 &= 2\nu_0 (\nabla_j v_i) (\nabla_j v_l) (\nabla_l v_i) \\ T_2 &= 2\nu_0^2 (\nabla_j \nabla_l v_i)^2. \end{aligned} \quad (11)$$

Equations (8)-(11) must be solved subject to initial and boundary conditions as well as the incompressibility constraint $\nabla \cdot \mathbf{v} = 0$. In order to derive equations for the mean values of K and \mathcal{E} , equations (8)-(11) must also be averaged over an ensemble of the fluctuating part of the velocity field \mathbf{v} . In the absence of a systematic averaging procedure, turbulence modellers have used intuitive reasoning combined with experimental data, tensorial and dimensional invariance, as well as scaling arguments based on the Kolmogorov theory³⁻⁶.

In the simple case of decaying turbulence with no mean velocity field, the equation of motion for the mean kinetic energy is usually written as:

$$\frac{\partial \bar{K}}{\partial t} = -\bar{\mathcal{E}} + \frac{\partial}{\partial x_i} \left(\alpha_K \nu \frac{\partial \bar{K}}{\partial x_i} \right) \quad (12)$$

where $\nu = \nu_0 + \nu_T$ is the total viscosity and α_K is a proportionality constant. The derivation of the equation for $\bar{\mathcal{E}}$ is more difficult since it is easily shown that both T_1 and T_2 in (11) are $O(Re_t^{1/2})$ where $Re_t \equiv \bar{K}^2 / \nu_0 \bar{\mathcal{E}} = O(u_{rms} L / \nu_0)$ is the turbulence Reynolds number. However,

the following bold assumption (cf. Tennekes and Lumley⁷) is fruitful: it is assumed that the singular contributions to T_1 and T_2 cancel each other in the limit as $Re_t \rightarrow \infty$ and the remaining $O(1)$ part can be written as

$$T_1 + T_2 = C_{\varepsilon 2} \frac{\bar{\mathcal{E}}^2}{\bar{K}} \quad (13)$$

where $C_{\varepsilon 2} = O(1)$. Thus, in decaying turbulence:

$$\frac{\partial \bar{\mathcal{E}}}{\partial t} = -C_{\varepsilon 2} \frac{\bar{\mathcal{E}}^2}{\bar{K}} + \frac{\partial}{\partial x_i} \left(\alpha_{\varepsilon} \nu \frac{\partial \bar{\mathcal{E}}}{\partial x_i} \right) \quad (14)$$

where $\alpha_{\varepsilon} = O(1)$. The assumption (13) was not rigorously justified but it has led to simple equations useful for practical calculations. In the case of homogeneous isotropic turbulence the diffusion terms in (12) and (14) disappear yielding

$$\bar{K} \propto t^{-\gamma} \quad (15)$$

where $\gamma = 1/(C_{\varepsilon 2} - 1)$. The fact that the coefficient $C_{\varepsilon 2}$ determines the power law of turbulence decay demonstrates the significant role of dimensionless constants in the theory of turbulence. Indeed, even a small error in $C_{\varepsilon 2}$ is amplified in the limit as $t \rightarrow \infty$. The first term on the right side of (14) has a simple interpretation in terms of a relaxation time:

$$\frac{\bar{\mathcal{E}}^2}{\bar{K}} = \frac{\bar{\mathcal{E}}}{T}$$

where

$$T = \frac{\bar{K}}{\bar{\mathcal{E}}}$$

is the only turbulence time-scale that one can construct from the parameters of the problem.

In flows with non-zero values of the mean strain $S_{ij} = \frac{1}{2}(\frac{\partial U_i}{\partial x_j} + \frac{\partial U_j}{\partial x_i})$, the velocity field in (8)-(11) can be decomposed into mean (\mathbf{U}) and fluctuating (\mathbf{u}) components. In this case the equations of motion are typically taken to be of the form:

$$\frac{\partial \bar{K}}{\partial t} + \mathbf{U} \cdot \nabla \bar{K} = -\tau_{ij} S_{ij} - \bar{\mathcal{E}} + \frac{\partial}{\partial x_i} \left(\alpha_K \nu \frac{\partial \bar{K}}{\partial x_i} \right) \quad (16)$$

$$\frac{\partial \bar{\mathcal{E}}}{\partial t} + \mathbf{U} \cdot \nabla \bar{\mathcal{E}} = -C_{\varepsilon 1} \frac{\bar{\mathcal{E}}}{\bar{K}} \tau_{ij} S_{ij} - C_{\varepsilon 2} \frac{\bar{\mathcal{E}}^2}{\bar{K}} + \frac{\partial}{\partial x_i} \left(\alpha_{\varepsilon} \nu \frac{\partial \bar{\mathcal{E}}}{\partial x_i} \right)$$

where $\tau_{ij} = \bar{u}_i \bar{u}_j$ is the Reynolds stress tensor and the coefficients $C_{\varepsilon 1}$ and $C_{\varepsilon 2}$ are constants that are usually determined from benchmark experiments. The $\bar{\mathcal{E}}$ - production term in (16) comes from the contributions to the $\bar{\mathcal{E}}$ - equation (10) of the type:

$$2\nu_o \frac{\partial u_i}{\partial x_l} \frac{\partial u_j}{\partial x_l} S_{ij}$$

which are modeled as

$$C_{\epsilon 1} \tau_{ij} S_{ij} / T$$

in the relaxation time approximation.

There are also dynamical constraints that a consistent turbulence model *must* obey. First of all, it is obvious that

$$\bar{K} \geq 0, \quad \bar{\mathcal{E}} \geq 0. \quad (17)$$

It can be shown that the conditions of realizability (17) are satisfied for homogeneous turbulent flows if:

$$\frac{d\bar{K}}{dt} \geq 0, \quad \frac{d\bar{\mathcal{E}}}{dt} \geq 0$$

when

$$\bar{K}, \bar{\mathcal{E}} \rightarrow 0.$$

Secondly, the turbulence model must be invariant under the Galilean transformation:

$$\mathbf{x}^* = \mathbf{x} - \mathbf{U}_0 t \quad (18)$$

where \mathbf{U}_0 is any constant velocity. In this sense, the turbulence model must behave like the original Navier-Stokes equations which are Galilean invariant. Any model violating invariance under (18) is physically incorrect.

Using the simplest closure for the deviatoric part of τ_{ij} :

$$\bar{\tau}_{ij} = -2\nu_T S_{ij} = -2C_\mu \frac{\bar{K}^2}{\bar{\mathcal{E}}} S_{ij} \quad (19)$$

(where $C_\mu \approx 0.085$ is a constant) (16) is transformed into a familiar form. It can be shown that (16) with (19) satisfies the realizability conditions $\bar{K} \geq 0$ and $\bar{\mathcal{E}} \geq 0$ provided that $C_{\epsilon 2} \geq 1$ and $C_\mu \geq 0$. These and other interesting properties of equations (16) and (19) have been recently reviewed by Speziale⁸.

Let us introduce the dimensionless variables

$$\eta = \frac{S\bar{K}}{\bar{\mathcal{E}}}; \quad K^* = \frac{\bar{K}}{\bar{K}_0}$$

where $S = (2S_{ij}S_{ij})^{1/2}$ and K_0 is the initial turbulent kinetic energy. In homogeneous shear flow where $\nabla^2 \bar{K} = \nabla^2 \bar{\mathcal{E}} = 0$, equations (16) and (19) have the simple form:

$$\begin{aligned} \frac{dK^*}{dt^*} &= K^*(C_\mu \eta - \eta^{-1}) \\ \frac{d\eta}{dt^*} &= -C_\mu (C_{\epsilon 1} - 1)\eta^2 + (C_{\epsilon 2} - 1) \end{aligned} \quad (20)$$

where $t^* = St$. Equation (20) has a single fixed point given by

$$\eta_0 = \left[\frac{C_{\varepsilon 2} - 1}{C_\mu(C_{\varepsilon 1} - 1)} \right]^{1/2} \quad (21)$$

which is obtained by setting $d\eta/dt = 0$. This fixed point yields asymptotic solutions for \bar{K} and $\bar{\mathcal{E}}$ of the form

$$\bar{K} \propto e^{\lambda t^*}, \quad \bar{\mathcal{E}} \propto e^{\lambda t^*}$$

where the growth rate λ is given by⁸

$$\lambda = \left[\frac{C_\mu(C_{\varepsilon 2} - C_{\varepsilon 1})^2}{(C_{\varepsilon 1} - 1)(C_{\varepsilon 2} - 1)} \right]^{\frac{1}{2}}. \quad (22)$$

Physical and numerical experiments on homogeneous shear flow – for not too large values of the dimensionless shear rate η – indicate that indeed, $\eta \rightarrow \eta_0$ and $\bar{K}, \bar{\mathcal{E}} \propto e^{\lambda t^*}$ for $t^* \gg 1$. This means that the solutions of any turbulence model must be attracted to this fixed point when η is not too large. The fact that the simple $\bar{K} - \bar{\mathcal{E}}$ model is capable of describing such a non-trivial behavior is remarkable.

Another important consequence of equations (16) and (19) is the Reynolds number independence of the von Karman constant in turbulent channel flow. It is easy to show that the normalized dimensionless velocity profile U^+ is given in the region of constant energy K^+ by:

$$U^+ = \frac{1}{\kappa} \ln y^+ + B \quad (23)$$

where κ is the von Karman constant. The dimensionless variables y^+ and U^+ will be discussed in more detail in Section IV. It follows from the model (16) and (19) that the von Karman constant is independent of Re . This is the result of the cancellation of the singular terms assumed in the derivation of (13). If, on the other hand $T_1 + T_2 = O(Re_t^{1/2})$ and the assumption (13) is incorrect, then the von Karman constant κ and the constant B in (23) will depend on Re_t . This would have a significant impact on engineering calculations since (23) enters in the expression for the friction coefficient. Surprisingly, even today, there is no compelling experimental evidence for the constancy of B and κ , although the prevailing opinion is that B and κ are constants.

Now let us discuss the closure assumption (19), which can be rewritten as:

$$\bar{\tau}_{ij} = -2C_\mu K \eta_{ij} \quad (24)$$

where $\eta_{ij} = S_{ij} \bar{K}/\bar{\mathcal{E}}$ is a dimensionless tensor which is equal to zero in isotropic turbulence. When η_{ij} is small, the deviation from the isotropic solution is small. Unfortunately, in many

practical applications of the $\bar{K} - \bar{\mathcal{E}}$ model, like channel flow, the values of parameter η_{ij} vary from $\eta \simeq 20$ in the buffer region to $\eta \simeq 3$ in the logarithmic layer (where $\eta \equiv \|\eta_{ij}\|$).

The dimensionless tensor η_{ij} can be used for a perturbation expansion of $\bar{\tau}_{ij}$ in powers of η when the departures from isotropy are small:

$$\bar{\tau}_{ij} = -K[2C_\mu\eta_{ij} + O(\eta_{ij}^2) + \dots]. \quad (25)$$

In this case, the theory of strained turbulence can be formulated in terms of a double expansion in powers of the two dimensionless small parameters Re^{-1} and η_{ij} . This expansion gives rise to the anisotropic eddy viscosity explored by Speziale⁹ and Rubenstein and Barton¹⁰. The existence of the second dimensionless expansion parameter η is not reflected in the functional form of the standard $\bar{K} - \bar{\mathcal{E}}$ model. This may account for the relatively poor performance of the standard model in flows with large values of η_{ij} .

It is apparent that a systematic derivation of turbulence models will enable us to address some of following questions:

- (i) Is it true that $T_1 + T_2 = O(1)$ as in (13)?
- (ii) Does the model (16) include all of the relevant effects or is something missing?
- (iii) Is it possible to derive a more complete Galilean invariant model than (16) satisfying the constraints discussed above, namely:
 - (a) $K \geq 0; \mathcal{E} \geq 0$ (realizability)
 - (b) $d\eta/dt = 0$ when $\eta \rightarrow \eta_o$ (fixed point)
 - (c) $\kappa = O(1)$?

Condition 3(a) and the requirement of Galilean invariance are the basic constraints, while constraints 3(b)-(c) are based on experimental data and must be accepted with some measure of skepticism until theoretically justified.

II. Renormalization Group Methods and Turbulence Models

The equations of motion (8)-(11) describe general turbulent flow. We assume that the turbulence is driven by mean strains and decompose the velocity field into mean and fluctuating parts ($\mathbf{v} = \mathbf{U} + \mathbf{u}$) as in Section I. We also make the basic assumption that the turbulence statistics are homogeneous when the mean strain S_{ij} is not too large. Next, we assume that the fluctuating velocity field \mathbf{u} is governed by the Navier-Stokes equations driven

by a random force, chosen in such a way that the global properties of the resulting field are the same as those in the flow driven by the mean strain S_{ij} .

To derive the equations for \mathbf{u} , we consider an infinite domain in which a Newtonian fluid is stirred by a Gaussian random force. The force is defined by its correlation function in wavevector and frequency space (see Yakhot and Orszag²),

$$\begin{aligned} \langle f_i(\mathbf{k}, \omega) f_j(\mathbf{k}', \omega') \rangle &= 2D_0(2\pi)^{d+1} k^{-y} P_{ij}(k) \delta(k + k') \delta(\omega + \omega'), \quad \Lambda_L < k < \infty \\ &= 0, \quad \Lambda_s < k \leq \Lambda_L \end{aligned} \quad (26)$$

where \mathbf{k} is the wavevector, ω is the frequency, $k = |\mathbf{k}|$ and d is the number of space dimensions. The parameter y is chosen to give the Kolmogorov form of the small scale energy spectrum; and in three dimensions $y = d = 3$. Statistical homogeneity in space and time is guaranteed through the factors $\delta(k + k')\delta(\omega + \omega')$ in (26). The projection operator $P_{ij}(k) = \delta_{ij} - k_i k_j / k^2$ makes the force statistically isotropic and divergence-free. In the limit of infinite Reynolds numbers, $\Lambda_L \rightarrow 0$ (but $\Lambda_L \gg \Lambda_s \rightarrow 0$). The forcing function (26) reflects the fact that turbulence is usually driven by hydrodynamic instabilities with the most unstable mode at $k = \Lambda_L$. The traditional view is that this primary instability generates velocity fluctuations with $k > \Lambda_L$ such that there is a direct energy cascade to small scales. The energy cascade may itself generate a universal random force of the form (26), but this has not yet been demonstrated rigorously.

Our model is the forced Navier-Stokes equations:

$$\begin{aligned} \frac{\partial v_i}{\partial t} + v_j \nabla_j v_i &= -\nabla_i p + \nu_o \nabla^2 v_i + f_i \\ \nabla_i v_i &= 0 \end{aligned} \quad (27)$$

where the Gaussian force \mathbf{f} is given by (26) and the density ρ has been absorbed in the pressure p . In contrast to the earlier development of RNG models in Ref. (2), the only new feature of the model (26)-(27) is the infrared cutoff of the random force: $\langle f_i f_j \rangle = 0$ when $0 < k < \Lambda_L$. This property, which is usually unimportant, is needed if we wish to derive an equation for the mean rate of energy dissipation $\bar{\mathcal{E}}$.

The dynamical equations for the total kinetic energy per unit mass $K \equiv \frac{1}{2} v_i v_i$ and the homogeneous part of the instantaneous rate of energy dissipation per unit mass $\mathcal{E} \equiv \nu_o (\nabla_j v_i)^2$ are obtained from (27),

$$\frac{\partial K}{\partial t} + v_i \nabla_i K = -\mathcal{E} + \nu_o \nabla^2 K - \nabla_i (v_i p) + v_i f_i \quad (28)$$

$$\begin{aligned} \frac{\partial \mathcal{E}}{\partial t} + v_i \nabla_i \mathcal{E} &= 2\nu_o (\nabla_j v_i) (\nabla_j f_i) - 2\nu_0 (\nabla_j v_i) (\nabla_j v_l) (\nabla_l v_i) \\ &\quad - 2\nu_0^2 (\nabla_j \nabla_l v_i)^2 - 2\nu_0 (\nabla_j v_i) (\nabla_i \nabla_j p) + \nu_0 \nabla^2 \mathcal{E}. \end{aligned} \quad (29)$$

In the equation for \mathcal{E} , driven by large-scale features such as boundary and initial conditions, T_1 balances T_2 to leading order. As we shall see, for steady-state flows (27)-(29) is sustained by the force \mathbf{f} ; T_2 is balanced by both T_1 and the random-force contribution to the \mathcal{E} -production given by $P_{\mathcal{E}} = 2\nu_0(\nabla_j v_i)(\nabla_j f_i)$.

We seek equations for the mean values $\mathbf{U} \equiv \langle \mathbf{v} \rangle$, $\bar{K} = \langle K \rangle$ and $\bar{\mathcal{E}} \equiv \langle \mathcal{E} \rangle$, averaged over an ensemble of the *fluctuating* velocity field. To find these equations, we shall use the dynamic renormalization group and the ε -expansion. Since the renormalized equations for \bar{K} and $\bar{\mathcal{E}}$ may not be trivially related to the renormalized Navier-Stokes equations, the RNG procedure must be applied to all of the equations (27)-(29).

The renormalization group applied to (28)-(29) is described in detail in Yakhot and Smith¹¹. Here we present the main results. The equations of motion averaged over the fluctuating velocity field \mathbf{v} are:

$$\begin{aligned} \frac{\partial U_i}{\partial t} + \mathbf{U} \cdot \nabla U_i &= -\nabla_i p + \frac{\partial}{\partial x_j} \left[\nu \left(\frac{\partial U_i}{\partial x_j} + \frac{\partial U_j}{\partial x_i} \right) \right] \\ \frac{\partial \bar{K}}{\partial t} + \mathbf{U} \cdot \nabla \bar{K} &= -\bar{\mathcal{E}} - \bar{\tau}_{ij} S_{ij} + \frac{\partial}{\partial x_i} \left(\alpha_K \nu \frac{\partial \bar{K}}{\partial x_i} \right) \\ \frac{\partial \bar{\mathcal{E}}}{\partial t} + \mathbf{U} \cdot \nabla \bar{\mathcal{E}} &= -C_{\varepsilon 1} \frac{\bar{\mathcal{E}}}{\bar{K}} \bar{\tau}_{ij} S_{ij} - C_{\varepsilon 2} \frac{\bar{\mathcal{E}}^2}{\bar{K}} - \mathcal{R} + \frac{\partial}{\partial x_i} \left(\alpha_{\varepsilon} \nu \frac{\partial \bar{\mathcal{E}}}{\partial x_i} \right) \end{aligned} \quad (30)$$

where

$$\mathcal{R} = 2\nu_0 S_{ij} \frac{\overline{\partial u_i \partial u_i}}{\partial x_i \partial x_j}, \quad (31)$$

$C_{\varepsilon 1} = 1.42$, $C_{\varepsilon 2} = 1.68$, and $\alpha_K = \alpha_{\varepsilon} = 1.39$. The relations (30)-(31) are obtained in the lowest order of the effective Reynolds number:

$$\lambda_*^2 = Re_*^2 = \frac{2D_0}{\nu \Lambda_i^4} \propto \varepsilon \simeq O(1) \quad (32)$$

where $\Lambda_i = 2\pi/L$ and ν is the effective viscosity (7). The parameter $\varepsilon = 7 - y$ is characteristic of the random noise driving this artificial flow. It was also shown¹¹ that in this order of the expansion, $T_1 + T_2 = O(1)$ which confirms the hypothesis leading to (13). In sheared turbulence where $S_{ij} \neq 0$, the Reynolds decomposition generates contributions of the order

$$\nu_0 S_{ij} \frac{\overline{\partial u_i \partial u_i}}{\partial x_i \partial x_j}. \quad (33)$$

The isotropic and homogeneous random velocity field \mathbf{v} was assumed to be governed by the equations (2)-(4). The renormalization group and the ε -expansion were applied to evaluate (33). This systematic procedure generated an expansion in powers of the dimensionless parameter $\eta_{ij} = S_{ij} \bar{K} / \bar{\mathcal{E}}$. The contribution to \mathcal{R} in (31) is small for weakly

strained turbulence and large in the rapid distortion limit when $\eta \rightarrow \infty$. All attempts to close (31) using the methods based on the ε -expansion were fruitless. In the next section we shall show how to evaluate (31) by applying the general criteria outlined in Section I.

III. Generalized $\bar{K} - \bar{\mathcal{E}}$ model

Neglecting \mathcal{R} in (31) and using the low order closure (19) for $\bar{\tau}_{ij}$, we obtain equations of motion, which are those of the standard $\bar{K} - \bar{\mathcal{E}}$ model:

$$\begin{aligned}\frac{D\bar{K}}{Dt} &= 2\nu_T S_{ij}^2 - \bar{\mathcal{E}} + \frac{\partial}{\partial x_i} \left(\alpha_K \nu \frac{\partial \bar{K}}{\partial x_i} \right) \\ \frac{D\bar{\mathcal{E}}}{Dt} &= 2C_{\varepsilon 1} \frac{\bar{\mathcal{E}}}{\bar{K}} \nu_T S_{ij}^2 - C_{\varepsilon 2} \frac{\bar{\mathcal{E}}^2}{\bar{K}} + \frac{\partial}{\partial x_i} \left(\alpha_{\varepsilon} \nu \frac{\partial \bar{\mathcal{E}}}{\partial x_i} \right)\end{aligned}\quad (34)$$

where $D/Dt = \partial/\partial t + \mathbf{U} \cdot \nabla$.

This model satisfies all of the criteria formulated in Section I. In homogeneous shear flow where $\partial U_i / \partial x_j = S \delta_{i1} \delta_{j2}$, equations (34) have the fixed point $\eta_0 = \left[\frac{C_{\varepsilon 2} - 1}{C_{\mu} (C_{\varepsilon 1} - 1)} \right]^{1/2} \simeq 4.38$ and for $St \gg 1$ the kinetic energy and dissipation grow exponentially:

$$\frac{\bar{K}}{\bar{K}_0} \propto \frac{\bar{\mathcal{E}}}{\bar{\mathcal{E}}_0} \propto e^{\lambda t^*}$$

with a growth rate $\lambda = 0.142$, which is very close to that obtained from numerical and physical experiments. These results will be discussed in more detail in Section V.

The model (34) is based on the assumption that η is small; however, the numerical value of $\eta \approx 4.38$ does not satisfy this constraint. Furthermore, in the logarithmic region of a turbulent channel flow, the value of the dimensionless shear $\eta = S\bar{K}/\bar{\mathcal{E}} \simeq 3$ is also not small. This means that the contribution to Eq. (30) due to \mathcal{R} cannot be neglected there.

Iterating the expression for \mathcal{R} using the Navier-Stokes equations will generate a power series:

$$\mathcal{R} = \nu_T S^3 \sum_{n=0}^{\infty} r_n \left(\frac{S\bar{K}}{\bar{\mathcal{E}}} \right)^n \quad (35)$$

where $S = (2S_{ij}S_{ij})^{1/2}$. It is clear that when $S \rightarrow 0$, \mathcal{R} goes to zero faster than $\frac{\bar{\mathcal{E}}}{\bar{K}} \nu_T S^2$ and may be neglected in (30). To use (35) in the case of large shear, let us consider as a model only the subset of terms corresponding to the geometric series

$$\mathcal{R}^0 = \nu_T S^3 \sum_{n=0}^{\infty} (-\beta)^n \left(\frac{S\bar{K}}{\bar{\mathcal{E}}} \right)^{3n} = \frac{\nu_T S^3}{1 + \beta \eta^3}. \quad (36)$$

We do not know the values of the coefficients r_n and cannot evaluate the magnitude of $\mathcal{R} - \mathcal{R}^0$. However, this form of \mathcal{R}^0 is plausable since (36) implies that

$$\mathcal{R}^0 = O\left(\frac{\bar{\mathcal{E}}^2}{\bar{K}}\right)$$

for all values of η . Thus, \mathcal{R}^0 vanishes when $\mathcal{E} \rightarrow 0$, a constraint that also follows from the definition of \mathcal{R} given in (31), so that (36) maintains the satisfaction of the realizability conditions (17). Assuming that the fixed point value $\eta_0 \simeq 4.38$, obtained in the limit of small S_{ij} , is invariant to dropping all terms but those in (36) we postulate that:

$$\mathcal{R} = \frac{\nu_T S^3 (1 - \frac{\eta}{\eta_0})}{1 + \beta \eta^3}. \quad (37)$$

Equation (37) can be rearranged into the alternative form

$$\mathcal{R} = \frac{C_\mu \eta^3 (1 - \frac{\eta}{\eta_0})}{1 + \beta \eta^3} \frac{\bar{\mathcal{E}}^2}{\bar{K}} \quad (38)$$

from which it is clear that the crucial constraint that $\mathcal{R} \rightarrow 0$ as $\bar{\mathcal{E}} \rightarrow 0$ is satisfied. The limits of weak and strong strains can also be easily discerned from (38). It is clear that in the limit of weak strains where $\eta \rightarrow 0$:

$$\mathcal{R} \simeq C_\mu \eta^3 \frac{\bar{\mathcal{E}}^2}{\bar{K}} \rightarrow 0. \quad (39)$$

On the other hand, in the limit of strong strains where $\eta \rightarrow \infty$:

$$\mathcal{R} \simeq -\frac{C_\mu}{\beta} \frac{\eta}{\eta_0} \frac{\bar{\mathcal{E}}^2}{\bar{K}} \quad (40)$$

which becomes singular. From the definition of \mathcal{R} given in (31), it follows that

$$\mathcal{R} = 2\eta A_{ij} S_{ij}^* \frac{\bar{\mathcal{E}}^2}{\bar{K}} \quad (41)$$

where

$$A_{ij} = \frac{\nu_0 \frac{\partial u_i}{\partial x_i} \frac{\partial u_j}{\partial x_j}}{\varepsilon}, \quad S_{ij}^* = \frac{S_{ij}}{S}.$$

It is a simple matter to show that $\|A_{ij}\|_2 \leq \frac{2}{3}$ and $\|S_{ij}^*\|_2 \leq \frac{1}{2}$ so that in the limit as $\eta \rightarrow \infty$, it follows that $\mathcal{R} = O(\eta)$ consistent with (40). Furthermore, in the limit as $\mathcal{E} \rightarrow 0$, $\mathcal{R} \rightarrow 0$ as $O(\bar{\mathcal{E}}^2)$ and in the limit as $\eta \rightarrow 0$, $\mathcal{R} \rightarrow 0$ as $O(\eta^2)$ or $O(\eta^3)$ (which follows from local isotropy; c.f. Monin and Yaglom¹²). These results are generally consistent with (39).

It is clear that the model (38), while not rigorously derived by RNG methods, satisfies a variety of important consistency conditions that place severe constraints on the possible

functional form of \mathcal{R} . In particular, no finite number of terms in the series (35) can give the desired asymptotics. While the analyticity of $\mathcal{R}(\eta)$ in the limit as $\eta \rightarrow \infty$ is not necessary we choose to assume it for simplicity. If this is the case, then the postulate (38) for \mathcal{R} is quite reasonable.

IV. The von Karman Constant

The proposed model for \mathcal{R} given in (38) contains one undetermined constant β which will now be related to the von Karman constant. In order to do this, we rewrite the dissipation rate transport equation in the equivalent form

$$\frac{\partial \bar{\mathcal{E}}}{\partial t} + \mathbf{U} \cdot \nabla \bar{\mathcal{E}} = -C_{\varepsilon 1} \frac{\bar{\mathcal{E}}}{K} \bar{\tau}_{ij} S_{ij} - C_{\varepsilon 2} \frac{\bar{\mathcal{E}}^2}{K} + \frac{\partial}{\partial x_i} \left(\alpha_{\varepsilon} \nu \frac{\partial \bar{\mathcal{E}}}{\partial x_i} \right) \quad (42)$$

where the coefficient $C_{\varepsilon 2}^*$ is given by

$$C_{\varepsilon 2}^* = 1.68 + \frac{C_{\mu} \eta^3 \left(1 - \frac{\eta}{\eta_0}\right)}{1 + \beta \eta^3}. \quad (43)$$

In the log layer of a turbulent boundary layer the turbulence production $-\bar{\tau}_{ij} S_{ij} = \bar{\mathcal{E}}$ and, hence, $\eta = 1/\sqrt{C_{\mu}}$ which renders $C_{\varepsilon 2}^*$ constant. Furthermore, convection effects (i.e., $D\bar{\mathcal{E}}/Dt$) can be neglected and the mean velocity assumes the logarithmic form (23) where

$$y^+ = \frac{yu_{\tau}}{\nu}, \quad U^+ = \frac{U}{u_{\tau}}$$

and u_{τ} is the shear velocity. With these assumptions, it is a straightforward calculation to show that (42) yields the constraint¹³

$$\kappa = \left[\frac{(C_{\varepsilon 2}^* - C_{\varepsilon 1}) \sqrt{C_{\mu}}}{\alpha_{\varepsilon}} \right]^{\frac{1}{2}} \quad (44)$$

which establishes a direct relationship between the von Karman constant κ and the constant β in the model (38) for \mathcal{R} . It follows that when

$$\beta = 0.012$$

the von Karman constant $\kappa = 0.4$. Fortunately, κ is not very sensitive to variations in β (in applications, β can be varied between 0.01 and 0.015 with only small changes in κ). With this selection of β (and the fixed point $\eta_0 = 4.38$) we now have a closed model for \mathcal{R} . Since the model yields a log layer with a von Karman constant κ of 0.4, it will give good results for turbulent channel flow. The model will be subjected to a more severe wall-bounded flow test in Section VI where turbulent flow over a backward facing step will be considered.

V. Homogeneous Shear Flow and the Relaxation Time Approximation

In this section we report tests of the new model in homogeneous shear flow where an initially isotropic turbulence (with turbulent kinetic energy \bar{K}_0 and dissipation rate $\bar{\mathcal{E}}_0$) is, at time $t = 0$, subjected to a constant shear rate S with the corresponding mean velocity gradient tensor

$$\frac{\partial U_i}{\partial x_j} = S\delta_{i1}\delta_{j2}.$$

The model given by equations (19), (30), and (38) yields a simple set of coupled nonlinear ordinary differential equations since $\bar{K} = \bar{K}(t)$ and $\bar{\mathcal{E}} = \bar{\mathcal{E}}(t)$. The solution obtained for the time evolution of the turbulent kinetic energy is compared in Figure 1 with the large-eddy simulation of Bardina et al.¹⁴ Despite the fact that the model yields an excellent long-time growth rate for \bar{K} (i.e., the model predicts that $\lambda = 0.142$ in comparison to physical and numerical experiments¹⁵⁻¹⁶ which indicate that λ is in the range of 0.14 - 0.16), the early time values of \bar{K} are overpredicted. This results from the use of an eddy viscosity representation for $\bar{\tau}_{ij}$ which responds too quickly to the application of the shear at $t = 0$.

The early time behavior can be described more accurately when a relaxation time approximation is introduced. In this approximation, we allow the Reynolds stress $\bar{\tau}_{ij}$ to relax to the eddy viscosity model (19) as follows:

$$\frac{d}{dt}(\bar{\tau}_{ij} + 2\nu_T S_{ij}) = -C_{T_R} \frac{\bar{\mathcal{E}}}{\bar{K}}(\bar{\tau}_{ij} + 2\nu_T S_{ij}) \quad (45)$$

for homogeneous flows where C_{T_R} is a relaxation coefficient. It is a simple matter to show that as a direct consequence of (45)

$$\frac{d\bar{\tau}_{ij}}{dt} = -C_{T_R} \frac{\bar{\mathcal{E}}}{\bar{K}}\bar{\tau}_{ij} - 2C_\mu(C_{T_R} + C_{\epsilon 2} - 2)\bar{K}S_{ij} + O(S_{ij}^2). \quad (46)$$

When an initially isotropic turbulence is strained, Crow¹⁷ showed that

$$C_\mu(C_{T_R} + C_{\epsilon 2} - 2) = \frac{4}{15}$$

which yields $C_{T_R} \approx 3.5$. Eq. (46) gives a simple Reynolds stress transport model.

In addition to (45) for the relaxation time approximation, $\nu_T S^2$ should be replaced by the production $P = -\bar{\tau}_{ij}S_{ij}$ in Eq. (37) giving the relaxation model

$$\mathcal{R} = \frac{\frac{P}{\varepsilon}\eta\left(1 - \frac{\eta}{\eta_0}\right)\bar{\mathcal{E}}^2}{1 + \beta\eta^3} \frac{\bar{K}}{\bar{K}} \quad (47)$$

where for homogeneous shear flow $P = -\tau_{12}S$. When the eddy viscosity model (in which $P = 2\nu_T S_{ij}S_{ij}$) is introduced in (47), Eq. (37) is recovered.

In Figure 2, the time evolution of the turbulent kinetic energy in homogeneous shear flow obtained from the relaxation model (46) - (47) is shown. These results are in excellent agreement with the large-eddy simulation of Bardina et al.¹⁴ This is quite encouraging considering the fact that this relaxation model was calibrated independent of homogenous shear flow (i.e., it was calibrated by setting the value of the von Karman constant to 0.4 and by using the Crow result for plane strain turbulence).

VI. Turbulent Flow over a Backward Facing Step

Turbulent flow over a backward facing step is one of the standard test cases used to evaluate the performance of turbulence models in separated flows. The Kim, Kline and Johnston¹⁸ experimental test case will be considered here for the backstep problem. For this flow configuration, the expansion ratio (step height: outlet channel height) E is 1:3 and the Reynolds number $Re = 132,000$ based on the inlet centerline mean velocity and the outlet channel height (see Figure 3). We will use the data for this test case as updated by Eaton and Johnston¹⁹ for the 1980-81 AFOSR-HTTM Stanford Conference on Turbulence. Since the turbulence is statistically steady, we can use the simpler form of the model given by (37) (i.e., there is no need to incorporate relaxational effects). The mean turbulence equations are solved numerically by a finite volume method on a 200×100 variable mesh (see Thangam and Speziale²⁰ for more details on the numerical method). Inlet profiles for U , \bar{K} , and $\bar{\epsilon}$ are specified five step heights upstream of the step corner (a developing turbulent channel flow calculation is carried out that matches the experimental inlet mean velocity profiles of Eaton and Johnston¹⁹); conservative extrapolated outflow conditions are applied thirty step heights downstream of the step corner. Along the upper and lower walls, the law of the wall (23) with $\kappa = 0.4$ and $B = 5$ is used along with standard log layer boundary conditions for the kinetic energy and dissipation obtained from a production-equals-dissipation equilibrium hypothesis and the constraint of vanishing normal derivative of \bar{K} at the wall. It was demonstrated recently by Thangam and Speziale²⁰ that, provided the flow field is *well resolved*, the use of these law of the wall boundary conditions leads to only minimal errors.

Two sets of results will be presented based on the algebraic model (37) for \mathcal{R} : one set obtained by using the isotropic eddy viscosity model (19) and another obtained from the anisotropic eddy viscosity model of Speziale⁹ given by

$$\begin{aligned} \bar{\tau}_{ij} = & -2C_\mu \frac{\bar{K}^2}{\bar{\epsilon}} S_{ij} - 4C_D C_\mu^2 \frac{\bar{K}^3}{\bar{\epsilon}^2} (\overset{\circ}{S}_{ij} - \frac{1}{3} \overset{\circ}{S}_{kk} \delta_{ij} \\ & + S_{ik} S_{kj} - \frac{1}{3} S_{kl} S_{kl} \delta_{ij}) \end{aligned} \quad (48)$$

where $\overset{\circ}{S}_{ij}$ is the Oldroyd derivative of S_{ij} with convective effects neglected; C_D is a dimensionless constant which assumes a value of 1.68. For thin shear layers, this model is very similar to the anisotropic eddy viscosity model derived by Rubenstein and Barton¹⁰ based on RNG methods. This type of anisotropic eddy viscosity model is obtained when terms of order η_{ij}^2 are maintained in the expansion (25) for $\bar{\tau}_{ij}$.

In Figures 4(a)-(b), the computed mean velocity streamlines and mean velocity profiles obtained using the isotropic eddy viscosity model (19) are compared with the experimental data.¹⁹ Reattachment is predicted at $x_R/H \approx 6.6$, a result that is within 6% of the experimentally measured reattachment point $x_R/H \approx 7.0$. The computed turbulence intensity and turbulence shear stress profiles are compared with experimental data in Figures 5(a)-(b). The agreement is comparably good.

By combining the model (37) for \mathcal{R} with the anisotropic eddy viscosity model (48), even better results are obtained. In Figures 6(a)-(b), the predicted mean velocity streamlines and mean velocity profiles are shown to compare extremely favorably with the experimental data.¹⁹ The model predicts reattachment at $x_R/H \approx 7.0$ which is essentially the same as the experimental result. Furthermore, the model predicts a noticeable secondary separation bubble below the corner of the step consistent with experimental observations for this back-step flow. The agreement between the model predictions and the experimental data for the turbulence intensity and turbulence shear stress profiles is also excellent as shown in Figures 7(a)-(b). The quality of these predictions is quite remarkable for a two-equation model.

VII. Concluding Remarks

The renormalization group formalism of Yakhot & Orszag for the development of turbulence models has been supplemented with scale expansions for the Reynolds stress and production of dissipation terms. Here, the extra expansion parameter is taken to be $\eta = S\bar{K}/\bar{\mathcal{E}}$ which is ratio of the turbulent to mean strain time scale. For the Reynolds stress, this approach – which leads to the development of anisotropic eddy viscosity models as well as Reynolds stress transport models – is analogous to that introduced by Rubenstein and Barton.¹⁰ However, the present method is completely new for the modelling of the production of dissipation term \mathcal{R} which is neglected in most of the commonly used turbulence models. The interesting result for \mathcal{R} is that no finite order truncation of the expansion satisfies the necessary physical constraints; terms of all orders in the expansion must be retained. This complication eliminates the possibility of determining the model explicitly in closed form. However, a highly plausible form, with only one undetermined constant, is postulated here which satisfies all of the necessary physical constraints (i.e., realizability and consistency with

the weak and strong strain limits). The constant is calibrated by setting the von Karman constant κ to 0.4.

The new models have been tested for homogeneous shear flow and for flow over a backward facing step. Excellent results are obtained in both cases. For the case of homogeneous shear flow, the best results are obtained from the Reynolds stress transport model (i.e., the relaxational model discussed in Section V). On the other hand, excellent results are obtained with eddy viscosity models for the backstep problem. In all of these calculations, no *ad hoc* adjustments of the constants are made. The applications considered in the paper are restricted to simple shear flows since the current version of the dissipation rate transport equation has only been modelled to account for the effects of irrotational strains. Incorporation of the effects of rotational strains, which can be important in turbulent flows involving curvature or a system rotation, is a difficult task that has not yet been achieved. The reduction in the energy cascade that occurs in rotating isotropic turbulence and the stabilizing or destabilizing effects of rotations on homogeneous shear flow are but two examples.^{21,22} This more difficult problem of accounting for rotational strains using a comparable scale expansion technique will be the subject of a future study.

Acknowledgements

Two of the authors (VY and SAO) would like to acknowledge support from the Defense Advanced Research Projects Agency under Contract N00014-86-K-0759 and from the Office of Naval Research under Contracts N00014-82-C-0451 and N00014-90-C-0039.

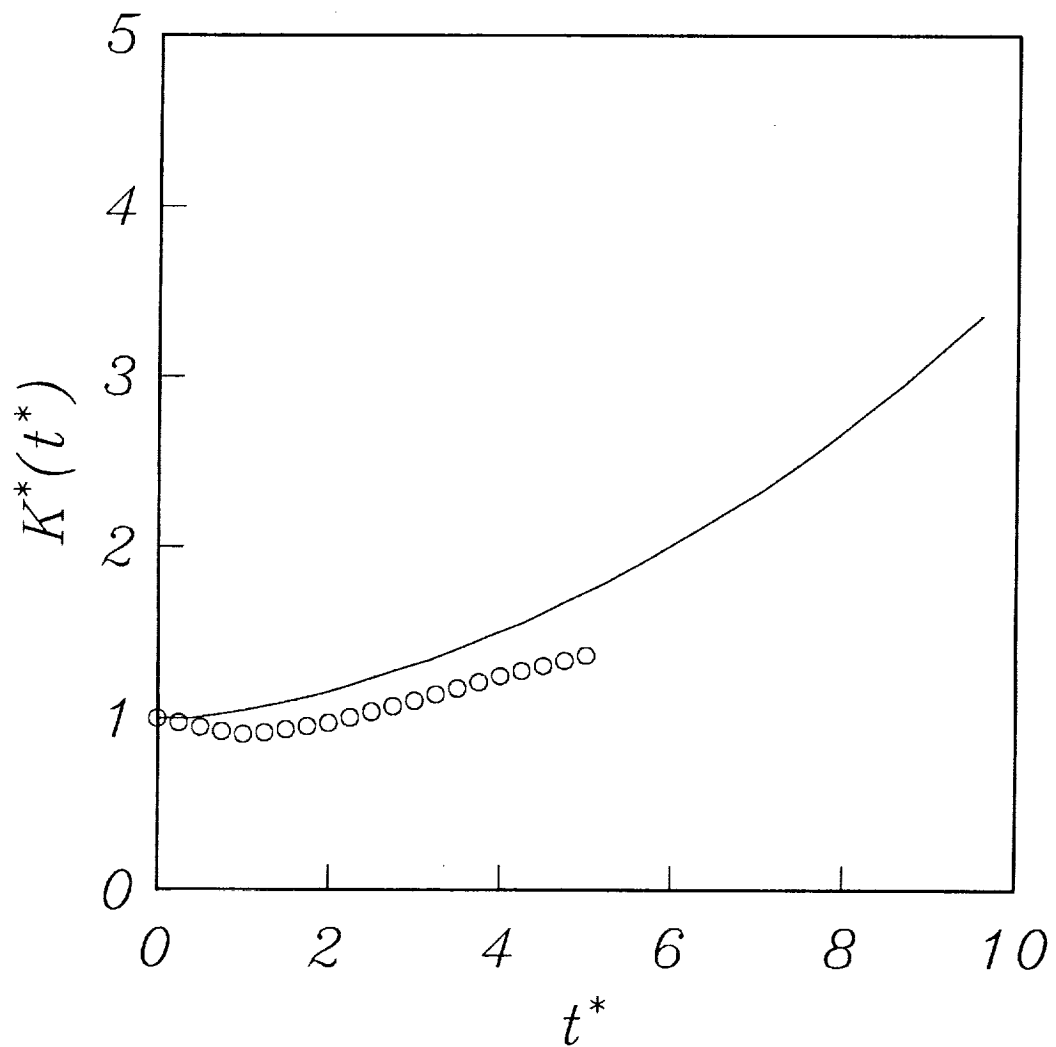
References

- ¹Kolmogorov, A. N. *Izv. Acad Sci. USSR, Phys.* **6**, 56 (1942).
- ²Yakhot, V. and Orszag, S. A. *J. Sci. Comp.* **1**, 3 (1986).
- ³Lumley, J. L. *Adv. Appl. Mech.* **18**, 123 (1978).
- ⁴Reynolds, W. C. *Lecture Notes for von Karman Institute. AGARD Lect. Ser. No. 86*, p. 1 (NATO, New York, 1987).
- ⁵Launder, B. E. and Spalding, D. B. *Comput. Methods Appl. Mech. Eng.* **3**, 269 (1974).
- ⁶Launder, B. E., Reece, G. J., and Rodi, W. *J. Fluid Mech.* **68**, 537 (1975).
- ⁷Tennekes, H. and Lumley, J. L. *A First Course in Turbulence* (MIT Press, Cambridge, MA, 1972).
- ⁸Speziale, C. G. *Ann. Rev. Fluid Mech.* **23**, 107 (1991).
- ⁹Speziale, C. G. *J. Fluid Mech.* **178**, 459 (1987).
- ¹⁰Rubenstein, R. and Barton, J. M. *Phys. Fluids A* **2**, 1472 (1990).
- ¹¹Yakhot, V. and Smith, L. M. *Phys. Fluids A*, submitted for publication.
- ¹²Monin, A. S. and Yaglom, A. M. *Statistical Fluid Mechanics: Mechanics of Turbulence*, Vol. 2 (MIT Press, Cambridge, MA, 1975).
- ¹³Patel, V. C., Rodi, W., and Scheuerer, G. *AIAA J.* **23**, 1308 (1985).
- ¹⁴Bardina, J., Ferziger, J. H., and Reynolds, W. C. *Stanford University Technical Report No. TF-19* (1983).
- ¹⁵Tavoularis, S. and Corrsin, S. *J. Fluid Mech.* **104**, 311 (1981).
- ¹⁶Rogers, M. M., Moin, P., and Reynolds, W. C. *Stanford University Technical Report TF-25* (1986).
- ¹⁷Crow, S. C. *J. Fluid Mech.* **33**, 1 (1968).
- ¹⁸Kim, J., Kline, S. J., and Johnston, J. P. *ASME J. Fluids Eng.* **102**, 302 (1980).
- ¹⁹Eaton, J. and Johnston, J. P. *Stanford University Technical Report MD-39* (1980).

²⁰Thangam, S. and Speziale, C. G. *AIAA J.*, to appear.

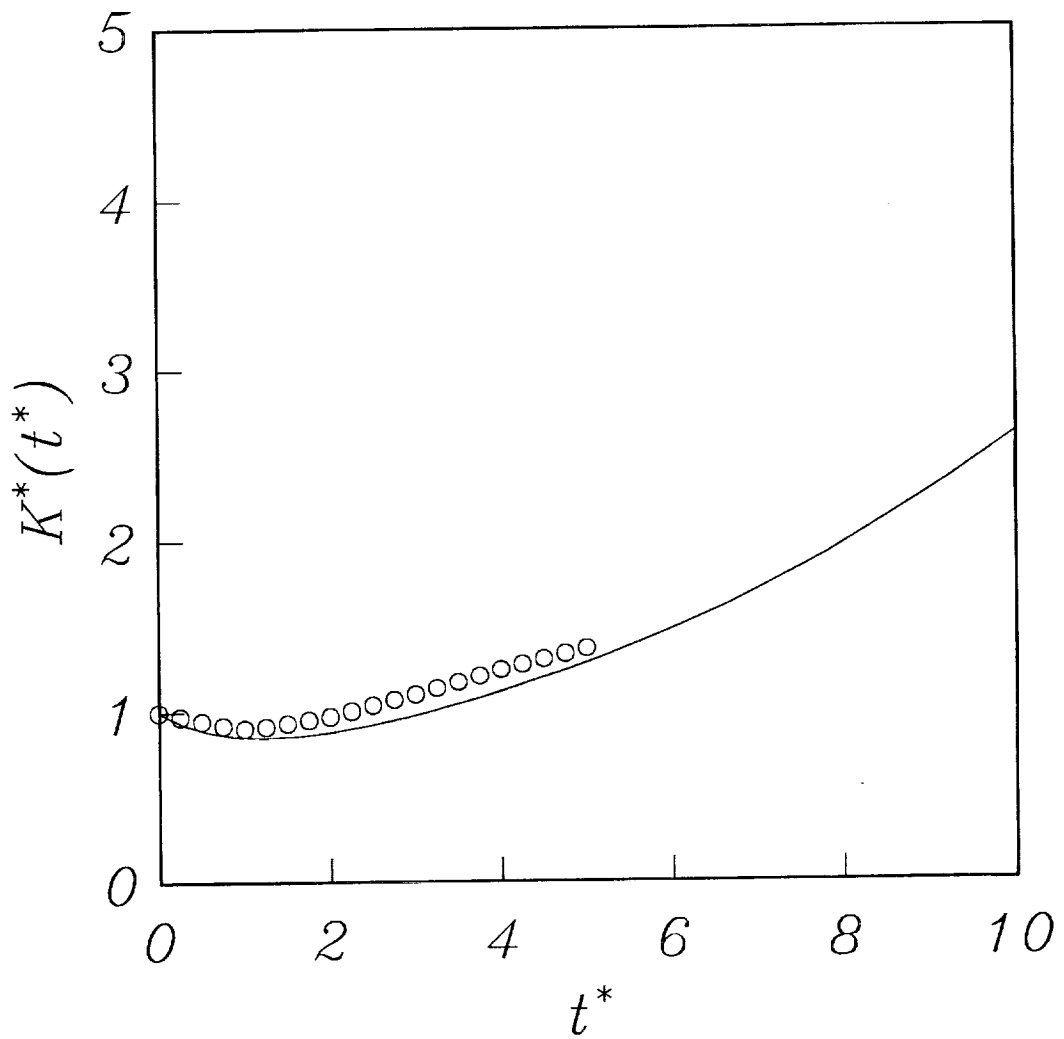
²¹Bardina, J., Ferziger, J. H., and Rogallo, R. S. *J. Fluid Mech.* **154**, 321 (1985).

²²Speziale, C. G. and Mac Giolla Mhuiris, N. *Phys. Fluids A* **1**, 294 (1989).



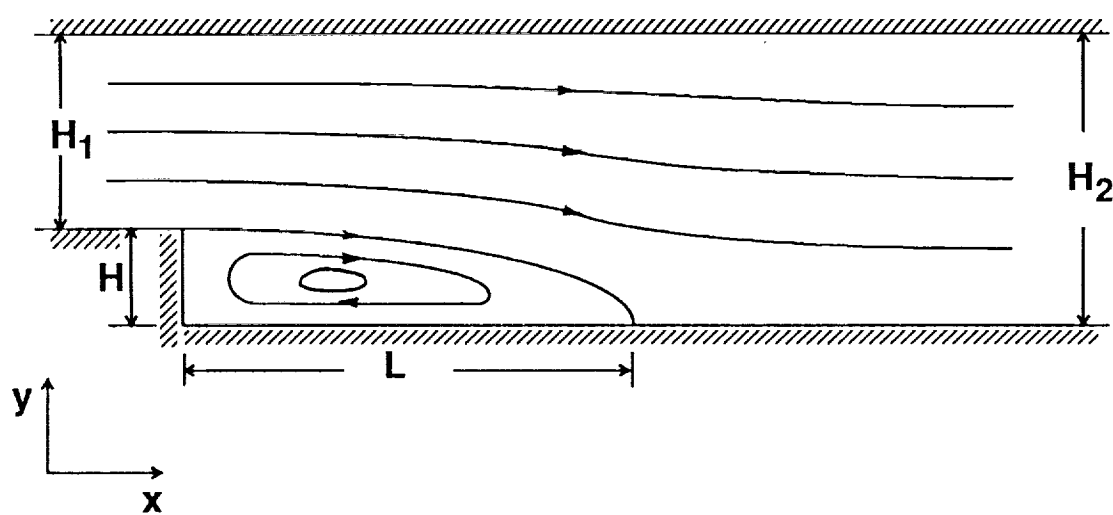
Time evolution of the turbulent kinetic energy in homogeneous shear flow.
 — K- ϵ model; o Large-eddy simulation of Bardina *et al.*¹⁴ for $\varepsilon_0/SK_0 = 0.296$

Figure 1



Time evolution of the turbulent kinetic energy in homogeneous shear flow.
 — Relaxation model; o Large-eddy simulation of Bardina *et al*¹⁴ for $\varepsilon_0/SK_0 = 0.296$

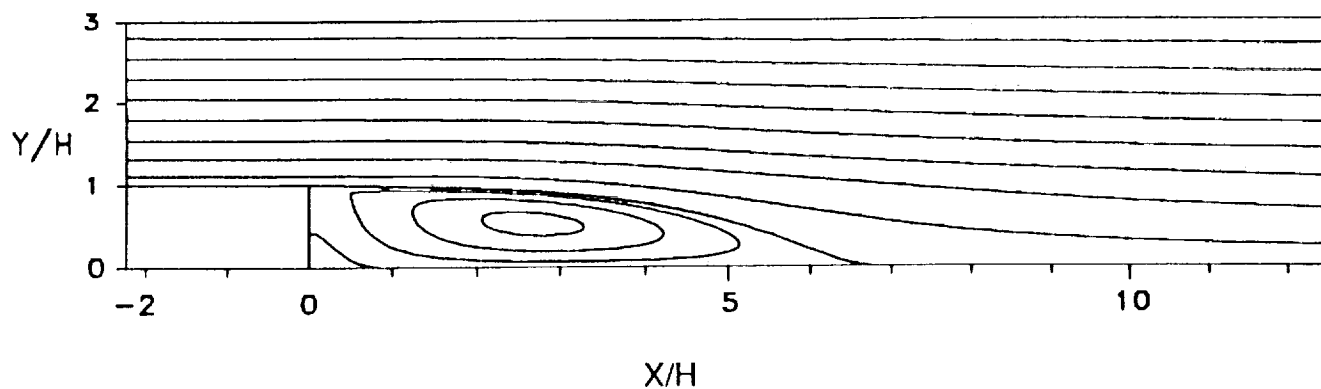
Figure 2



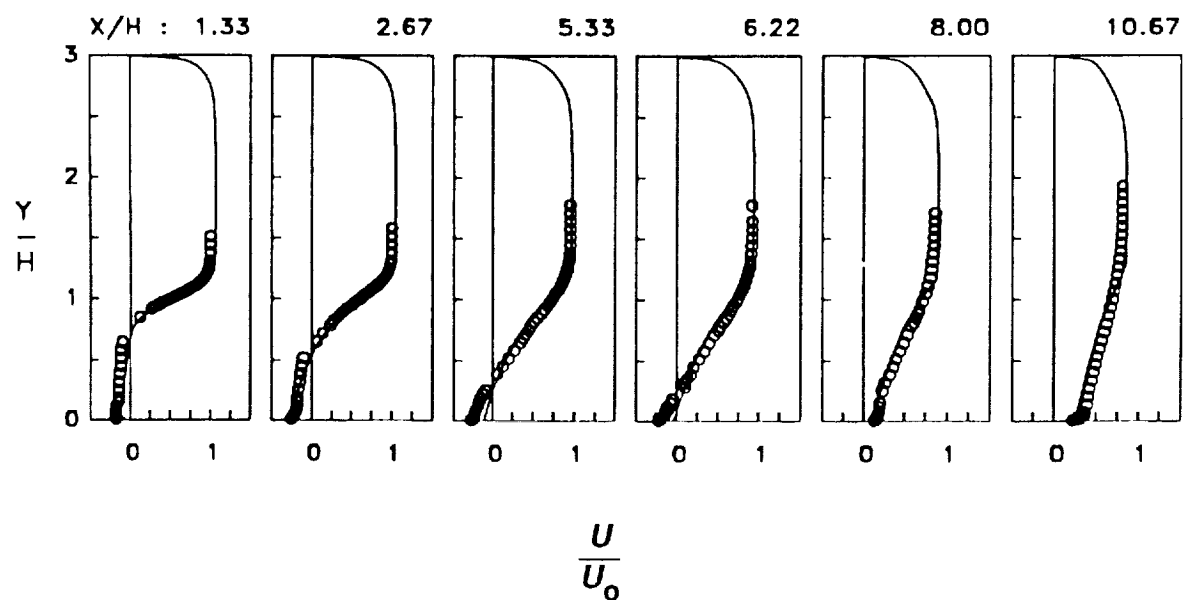
Turbulent flow over a backward facing step

Figure 3

BACKWARD-FACING STEP:



(a) Streamlines



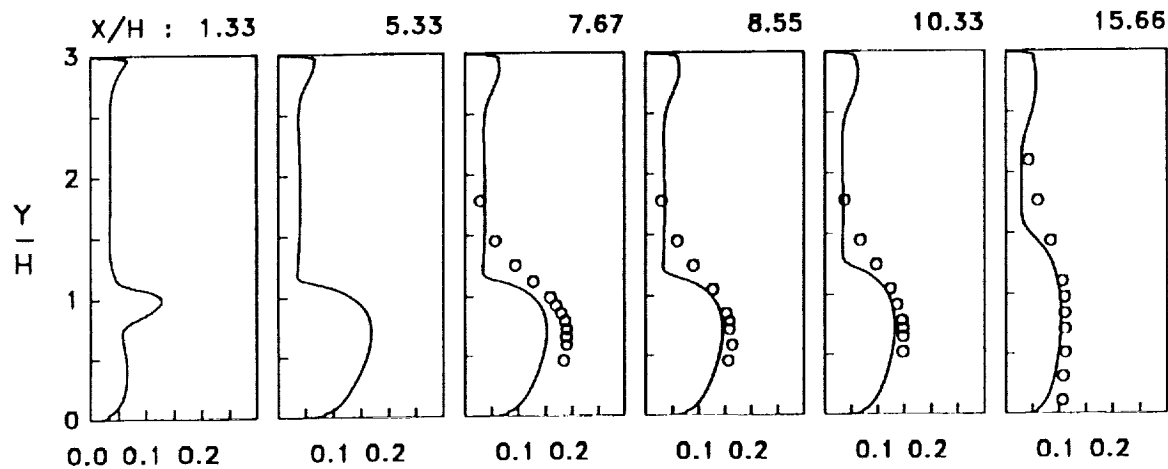
(b) Dimensionless mean velocity profile

(— Computations with isotropic eddy viscosity;
 o Experiments of Kim *et al*, 1980; Eaton & Johnston, 1981)

Computed mean flowfield for the new RNG $K-\epsilon$ model
 [$E = 1:3$; $Re = 132,000$; 200×100 mesh]

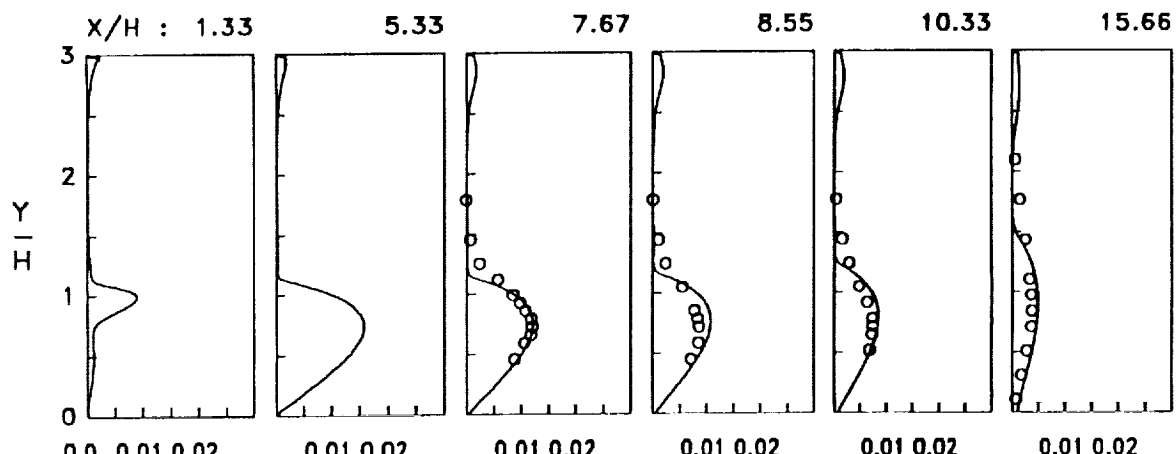
Figure 4

BACKWARD-FACING STEP:



$$\left(\frac{\overline{uu}}{U_0^2} \right)^{1/2}$$

(a) Turbulence Intensity



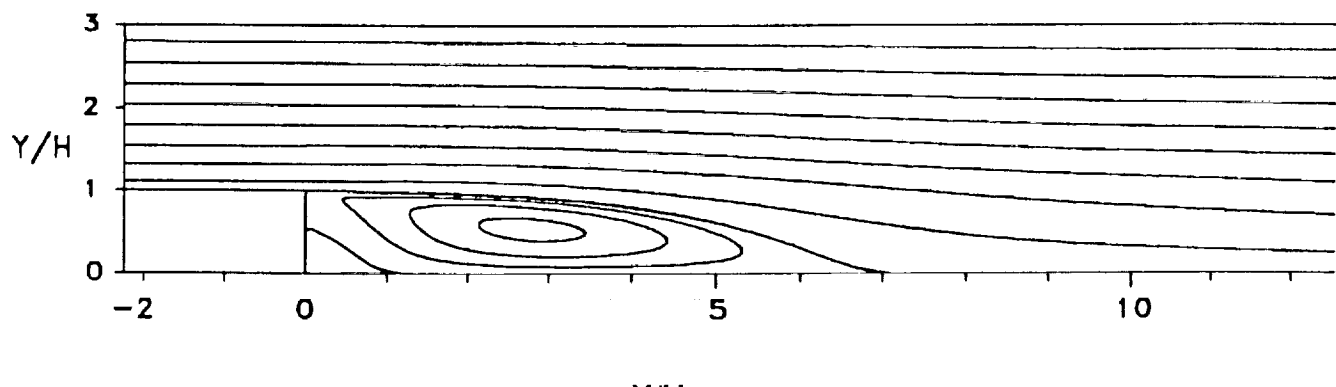
$$\left| \frac{\overline{uv}}{U_0^2} \right|$$

(b) Turbulence shear stress

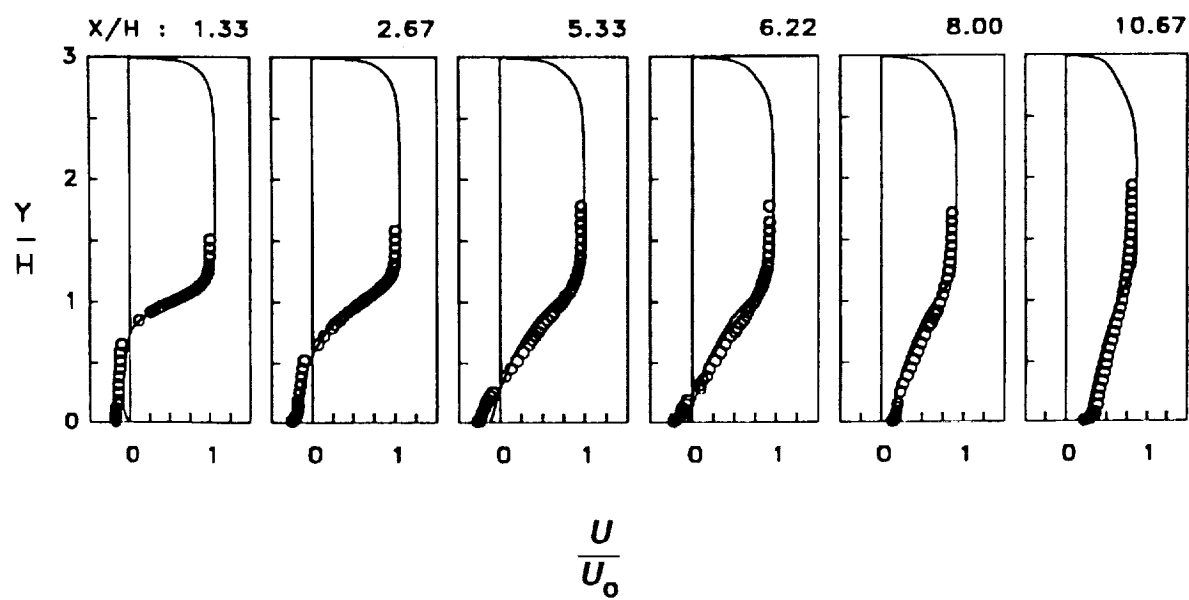
Computed turbulence stresses for the new RNG $K-\epsilon$ model [$E=1:3$; $Re = 132,000$; 200×100 mesh; — computations with isotropic eddy viscosity; o experiments of Kim *et al*, 1980; Eaton & Johnston, 1981]

Figure 5

BACKWARD-FACING STEP:



(a) Streamlines



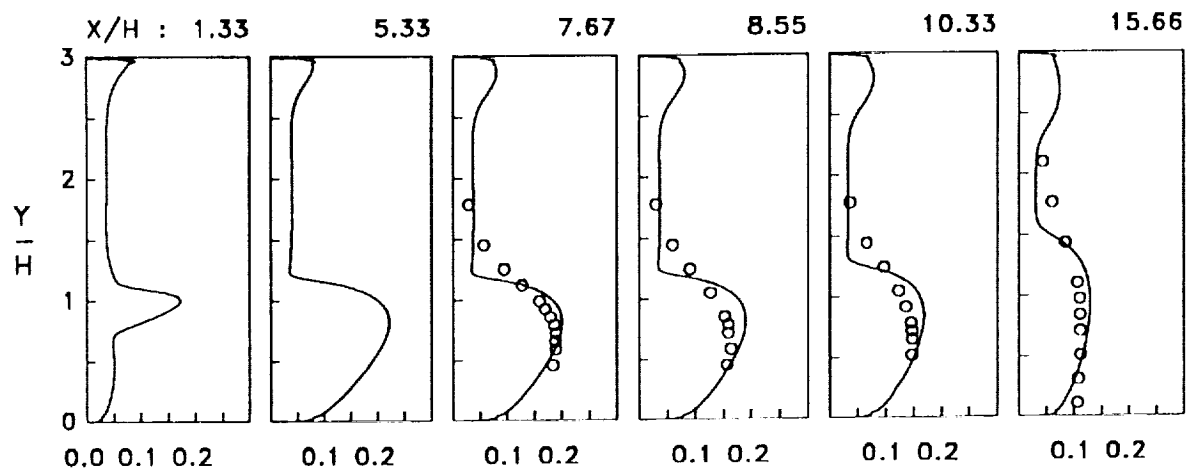
(b) Dimensionless mean velocity profile

(— Computations with anisotropic eddy viscosity;
 ○ Experiments of Kim *et al*, 1980; Eaton & Johnston, 1981)

Computed mean flowfield for the new RNG $K-\varepsilon$ model
 [E = 1:3; Re = 132,000; 200x100 mesh]

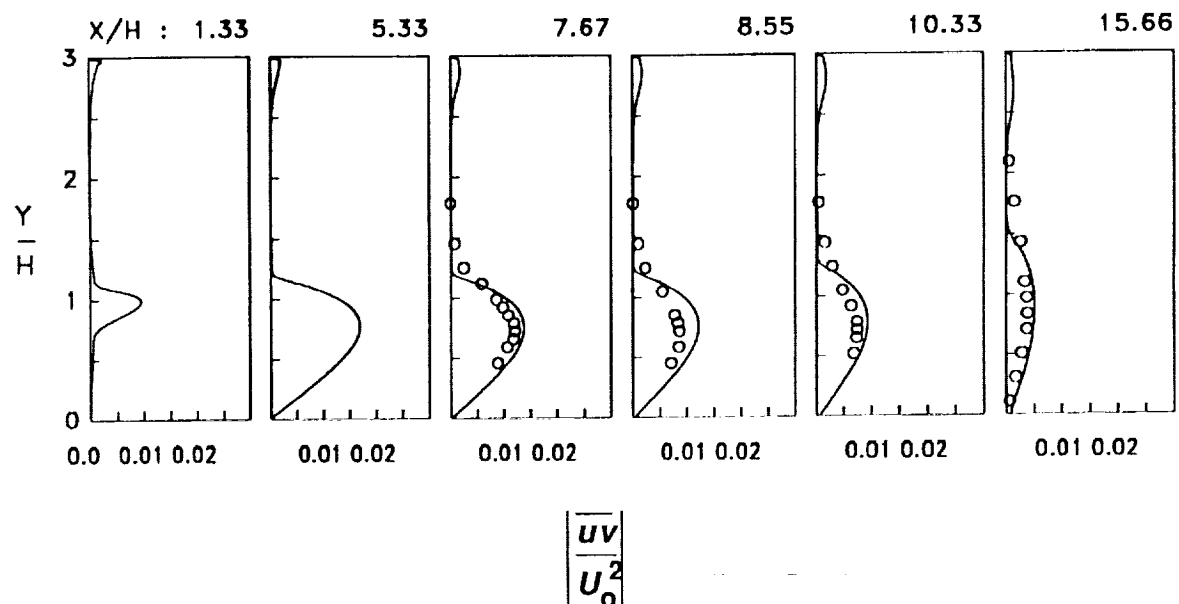
Figure 6

BACKWARD-FACING STEP:



$$\left(\frac{\overline{uu}}{U_0^2} \right)^{1/2}$$

(a) Turbulence intensity



(b) Turbulence shear stress

Computed turbulence stresses for the new RNG $K-\epsilon$ model [$E=1:3$; $Re = 132,000$; 200×100 mesh; — computations with anisotropic eddy viscosity; \circ experiments of Kim *et al*, 1980; Eaton & Johnston, 1981]

Figure 7



Report Documentation Page

